Food and Agriculture Organization of the United Nations

General Fisheries Commission for the Mediterranean

Sound monitoring baseline data report

Durrës, Albania
26 August–2 September 2023

By
Junio Fabrizio Borsani
Valentina Caradonna

This study was conducted within the framework of the "Fisheries and ecosystem-based management for the blue economy of the Mediterranean" (FishEBM-MED) project. Funded by the Global Environment Facility (GEF), the FishEBM-MED project is implemented by the Food and Agriculture Organization of the United Nations (FAO) and the United Nations Environment Programme (UNEP), with execution overseen by the General Fisheries Commission for the Mediterranean (GFCM) and the Mediterranean Action Plan|SPA/RAC.

gef

The GFCM Secretariat and the authors of this study warmly thank Arian Palluqi for his invaluable contributions, including the preparation and planning of the study, the facilitation of fieldwork, and his continuous support.

Index

Executive summary

The present report is intended to provide an initial assessment of potential impacts of underwater noise radiated from commercial shipping in Durrës Bay, Albania. Measurements of noise irradiated by two passenger ferries underway were taken. Predictions of irradiated noise from six ships at anchor were made. Analysis showed overall high levels of ambient noise. Due to local oceanographic conditions sound propagated with low attenuation in an intermediate spreading mode. Levels, duration and repetition patterns of irradiated noise suggested that no direct physical harm to fish can be foreseen. However, for three commercial species, namely the Hake, the Norway lobster and the common cuttlefish, reactions and physiological consequences related to stress can be predicted. With the necessity of finding both temporal and spatial mitigation options, a definition of entry and leave routes for ships as well as speed limits are suggested.

1. Introduction

In the context of the GEF Project Fisheries and Ecosystem Based Management for the Blue Economy of The Mediterranean (FISHEBM MED) a study on underwater noise pollution in Albania was executed. The study investigated acoustic risk components, such as commercial shipping. Physical properties of eight specific sources were investigated. Oceanographic parameters that are crucial for the assessment of local soundscapes were determined.

Several commercial fish species are sensitive to underwater sound. Goal of this study was to assess potential impacts derived from commercial shipping on fish and other marine fauna.

2. Terminology

Technical terminology cited in this report refers to ISO 18405:2017 (www.iso.org/obp/ui/#iso:std:iso:18405:ed-1:v1:en). We refer to ISO 13261-2:1998 only for the one-third octave band definition (https://www.iso.org/obp/ui/#iso:std:iso:13261:-2:ed-1:v1:en). Definition of metrics is reported in Table 1.

Metric	Definition
Root-mean-square sound pressure level, sound pressure level, SPL, L_p	Ten times the logarithm to the base 10 of the ratio of the *mean-square sound pressure* to the specified reference value, ${p_0}^2$, in decibels $$L_{p,rms} = 10log_{10}\left(\frac{p^2}{{p_0}^2}\right) dB$$ In underwater acoustic the reference pressure value of the mean-square sound pressure, ${p_0}^2$, is $1\mu Pa^2$. The reference value shall be specified.
Zero-to-peak sound pressure	Greatest magnitude of the *sound pressure* during a specified time interval, for a specified frequency range
Peak sound pressure level	Twenty times the logarithm to the base 10 of the ratio of the *zero-to-peak sound pressure*, p_{pk}, to the specified reference value, p_0, in decibels $$L_{p,pk} = 20log_{10}\left(\frac{p_{pk}}{p_0}\right) dB$$

	In underwater acoustic the reference pressure value of zero-to-peak sound pressure, p_0, is 1 µPa. The reference value shall be specified.
One-third-octave band	Band of sound covering a range of frequencies such that the highest is the cube root of two (approximately 1,26) times the lowest (ISO 13261-2:1998)
Power spectral density (PSD)	Describes the power present in the signal as a function of frequency, per unit frequency. Power spectral density is commonly expressed in watts per hertz (W/Hz).
Source level	Ten times the logarithm to the base 10 of the ratio of the *source factor*, F_S, to the specified reference value, F_{S0}, in decibels. $$SL = 10\log\left(\frac{F_S}{F_{S0}}\right) dB$$ F_{S0}=1µPa^2
Propagation loss	Difference between *source level* in a specific direction, L_S, and *mean-square sound pressure level*, $L_p(x)$, at a specified position, x. $$N_{PL}(x) = L_S - L_p(x)$$ Propagation loss is expressed in decibels (dB).

Table 1. Table reporting the definition of technical terminology cited in this report.

3. Target underwater noise sources: commercial ships

The Underwater Radiated Noise (URN) of the following two ferries was recorded: "Rigel III", of Ventouris Ferries (Figure 1) and "AF Francesca", of Adria Lines (Figure 2). Table 2 summarizes their physical characteristics. Information was derived from VesselFinder (https://www.vesselfinder.com/it). The last column of Table 2 features the expected source level (SL) of observed ships, according to the formula given by MacGillivray and de Jong (2021). The source level in the table refers to the one-third octave bands centred at 63 Hz and 125 Hz, since they are the bands which must be considered to monitor continuous low frequency sounds, i.e. shipping noise, according to the Marine Strategy Framework Directive (Dekeling *et al*., 2014).

Ferry	**IMO**	**Gross Tonnage**	**Length overall (m)**	**Beam (m)**	**Cruising speed (knts)**	**Draft (m)**	**Expected SL (dB re µPa 1m)**
Rigel III	7807744	16405	136	24.2	13.4	5.2	171.04 (63.1 Hz) 173.05 (125.9 Hz)
AF Francesca	7602089	19811	147.97	25.4	12.9	5.8	170.78 (63.1 Hz) 172.79 (125.9 Hz)

Table 2. Table summarizing characteristics of ferries Rigel III and AF Francesca.

Figure 1. Image of ferry Rigel III

Figure 2. Image of ferry AF Francesca.

In addition to the moving ferries described above, several ships were anchored offshore Durrës harbour. Nearby vessels which were visible on radar during recording operations are listed in Table 3. As well as for the recorded ferries, the expected source level estimated after MacGillivray and de Jong (2021) of nearby ships is reported.

Ferry	IMO	Vessel type	Gross Tonnage	Length overall (m)	Beam (m)	Cruising speed (knts)	Draft (m)	Distance from receiver (nm)	Expected SL (dB re µPa 1m)
Graciano II	-	Fishing	-	17	6	6.7	3	12.1	142.2 (63 Hz) 145.0 (125 Hz)
X-Press Kaveri	9470765	Cargo	17280	171.99	27.6	13	8.5	2.22	165.1 (63 Hz) 160.5 (125 Hz)
MSC Caledonia II	9262546	Cargo	24918	188.3	27.68	5.8	6.4	2.63	144.8 (63 Hz) 140.3 (125 Hz)
Soumaya-J	7118870	Cargo	2397	88.52	13.85	10.5	4	2.71	153.8 (63 Hz) 149.2 (125 Hz)
Grace Felix	9391402	Tanker	23403	184.32	27.43	6.3	8.8	1.24	157.0 (63 Hz) 150.8 (125 Hz)
Petit Sarah	NA							12.5	

Table 3. List of ships anchored nearby the listening station.

4. Environmental data

For both recordings environment resulted to be “+” (i.e. wind <10knts), the own ship was silent, other ships produced low level noises.

Table 4 summarizes local physical-chemical parameters of water. Figure 3 represents the local temperature-depth profile.

Date	Time	Conductivity (mS/cm)	Depth (m)	Temperature (°C)	Salinity (PSU)	Density (kg m-3)	SV (m/s)
31/08/2023	10:41:22	57.415	7.61	24.515	38.661	1026.293	1537.32
31/08/2023	10:41:27	57.261	12.48	24.383	38.655	1026.350	1537.08

Table 4. Table reporting environmental data acquired on 31 August 2023 at local time of 10.41: Conductivity, Depth, Temperature, Salinity, Density and Sound Velocity (SV). Credits to Jasco.

According to environmental data reported above and following the NPL equation, the sound velocity for sensor depth at 10 m is 1537.42 m/s (T= 24.515°C, S=38.661‰). Jasco sound speed was validated with NPL equation for 7.61m depth (1537.38 m/s) for Durrës latitude.

$$c = 1402.5 + 5T - 5.44\,x\,10^{-2}T^2 + 2.1\,x\,10^{-4}T^3 + 1.33S - 1.23\,x\,10^{-2}ST + 8.7\,x\,10^{-5}ST^2 + 1.56\,x\,10^{-2}Z + 2.55\,x\,10^{-7}Z^2 - 7.3\,x\,10^{-12}Z^3 + 1.2\,x\,10^{-6}Z(\Phi - 45) - 9.5\,x\,10^{-13}TZ^3 + 3\,x\,10^{-7}T^2Z + 1.43\,x\,10^{-5}SZ$$

Formula of NPL equation. From http://resource.npl.co.uk/acoustics/techguides/soundseawater/

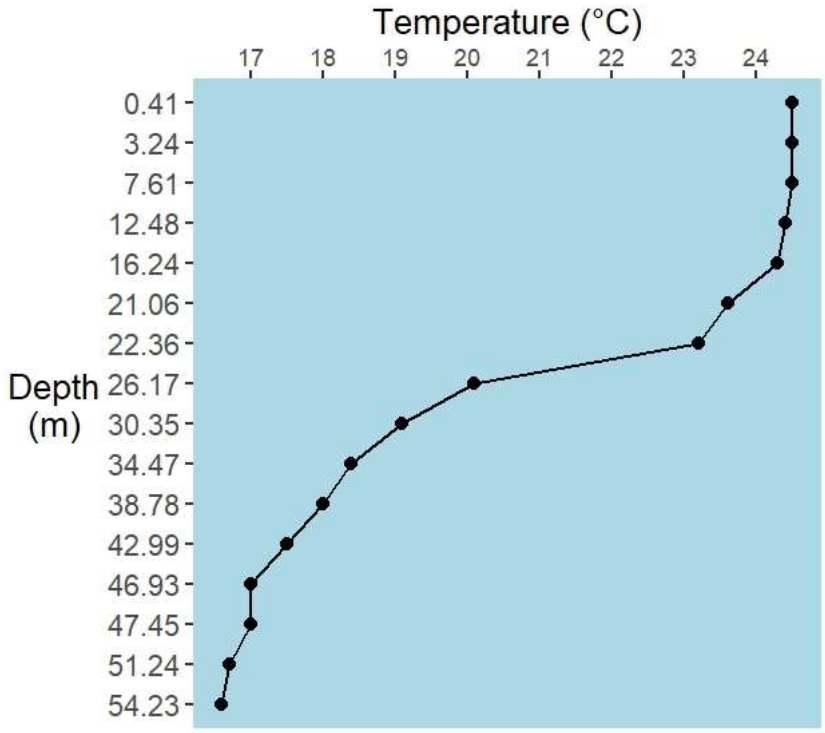

Figure 3. Figure showing the temperature-depth diagram, with a thermocline at approximately 25m depth.

5. Methods

5.1. Equipment

The recording chain consisted of:

- One hydrophone (TC4040-5)
- A voltage preamplifier (Reson VP1000)
- A digital recorder (TASCAM DR100 MK3)

Recording gain and amplifier gain were set to 12 dB and 32 dB respectively. High-pass filter was set to 10 Hz and recordings were mono-channel. Sample rate was 48 kHz and resolution was 24 bits. Figures 4 and 5 represent the instrumentation.

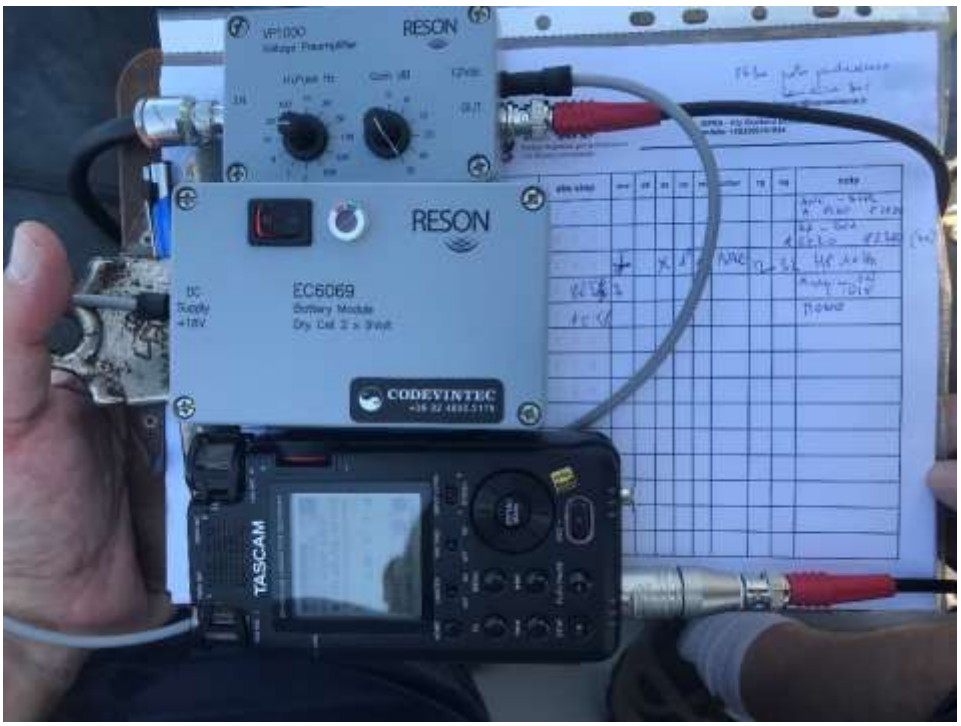

Figure 4. Instrumentation: from the top to the bottom there are preamplifier, its power supply and recorder. In the background the logs used to write down all ancillary information.

Figure 5. Picture of the hydrophone in its case and protection.

The recording chain was calibrated by comparison with a calibrated reference hydrophone, to obtain the receiving sensitivity for the entire chain and for different values of preamplifier gain. Since

recording channel calibration data are recorded in digital format, the results are expressed using a proper representation in terms of Scale Factor (SF) which applies to digital recording equipment for which traditional receiving sensitivity in V/Pa units (and related dB levels) cannot be defined. The SF can be viewed as the acoustic pressure in Pascal that corresponds to full scale in the output digital audio file: the higher the SF value, the lower the corresponding hydrophone sensitivity.

Table 5 summarizes the calibration results in terms of Scale Factor in pascal for the hydrophone for all its respective preamplifier gain settings. Our current setting was 32dB.

Gain (dB)	0	6	10	12	20	26	30	32	40	50
TC4040-5	126 808	63 555	-	31 853	12 681	6 355	-	3 185	-	-

Table 5. Calibration data of recording channels with hydrophone TC4040-5 in terms of Scale Factor (SF) in pascal, for respective preamplifier gain settings.

A RHIB vessel supplied by the Port Authority was used to reach the positions of the listening stations. A picture of it is shown in Figure 6.

Figure 6. Durrës Port Authority vessel used for the experiment.

5.2. Study area

The study area was immediately offshore Durrës port. We were positioned at locations with coordinates reported in Figure 6. We selected such positions to intercept ferries while entering the port. The rationale was to record all phases of the approach, from cruising speed to reduced speed regime, and to be as close as possible to the noise source.

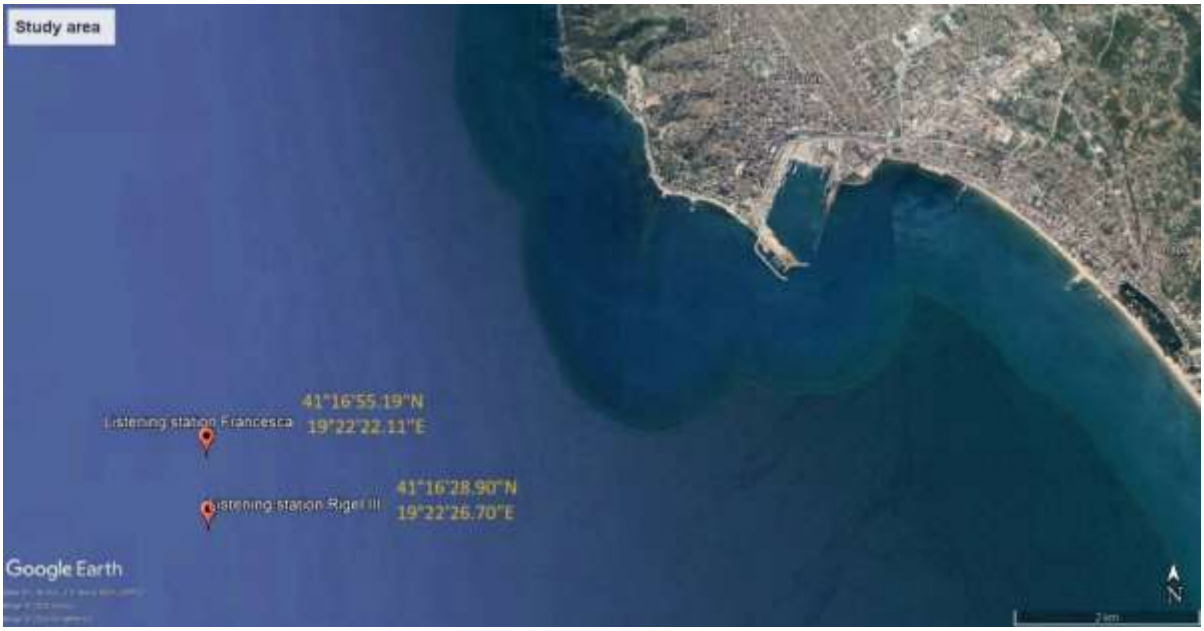

Figure 7. Figure showing the study area with the positions of our vessel, where acoustic measurements were carried out.

5.3. Data acquisition

Acoustic recordings were acquired during the morning of 1st September 2023, from 08.37 to 10.19. It was not possible to obtain additional data, because of adverse weather conditions characterizing the other days. In particular, strong wind resulted to be a relevant problem for obtaining recordings of sufficient quality. Timetables of Durrës ferries reduced the chance to acquire data, since at least half of the ferries arrived at hours where it was not possible to be at sea.

We succeed in obtaining acoustic files referring the passage of the two ships. An additional recording was made to characterize the local underwater soundscape without ships in motion in the immediate surroundings ("Blank").

Acoustic files were recorded in .wav format. Their duration is reported in Table 6.

File ID (.wav)	What	Duration (min.s)	Time (CEST)	Dimensions (KB)
230901_0059	Rigel III	7.05	08.37 - 08.44	59.780
230901_0060	Blank	6.01	08.50 – 08.57	50.741
230901_0061	AF Francesca	14.03	10.04 - 10.19	118.623

Table 6. Table reporting file durations and dimensions.

The hydrophone and cable were deployed near our vessel once the engine was turned off. The hydrophone was lowered at 10 m depth and 20 m away from the ship, with additional buoyancy (floater). The deployment scheme is represented in Figure 8 while a picture of the field setup is shown in Figure 9.

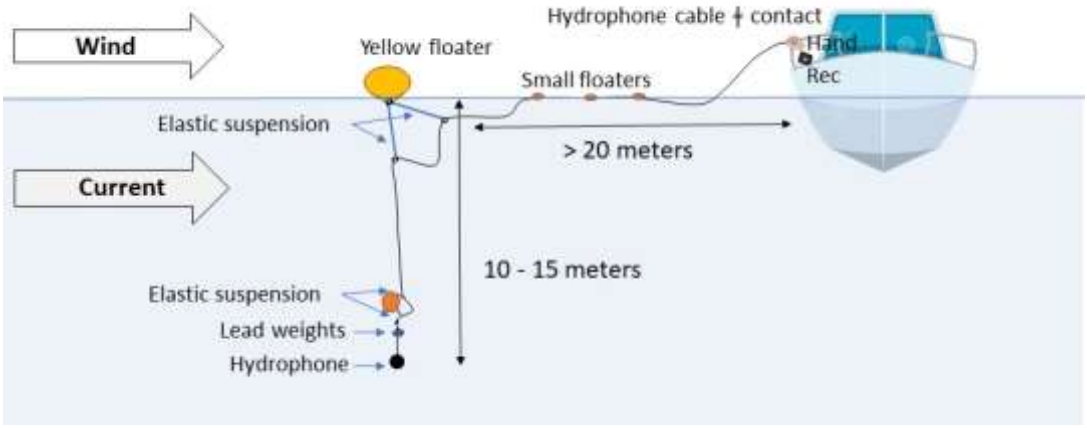

Figure 8. Scheme of deployment.

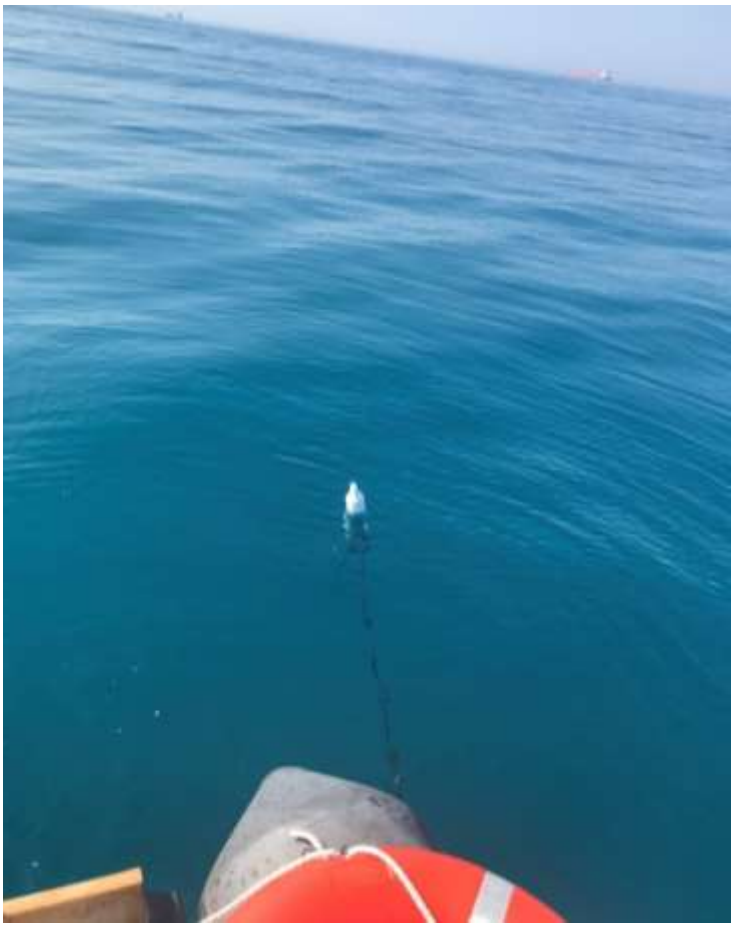

Figure 9. Picture of the floater which keeps the hydrophone away from the boat.

For both ferries the procedure was the same: we monitored the target ferry by radar. We kept track of a) the distance from us, b) the route, and c) the speed, so that we could position our boat as close as possible to the transient ferry. Once we had chosen the ideal position, we turned off the engine and lowered the hydrophone into the water, ready to record. When the ferry was close enough, we started recordings, in order to capture the ferry getting closer to the listening station, until the shortest distance among us (the listening station) and the vessel was reached. We stopped the recording when the ferry was again far enough. During recording activities, we kept track periodically of the distance among us and the vessel, to understand when the CPA was reached. The CPA is the Closest Point of Approach, i.e. the moment when the distance from receiver to noise source is shortest. Representations for both ferries passing by the listening station, with all points when the distances were noted, are Figure 10 and 11. Numerical data are reported in Table 7.

Figure 10. Figure reporting listening station and the progressive positions of the ferry Rigel III. For each position we measured the distance from the ferry to the boat, i.e. the listening station.

Figure 11. Figure reporting listening station and the progressive positions of the ferry AF Francesca. For each position we measured the distance from the ferry to the boat, i.e. the listening station.

Day	Ship name	Ship type	Station position	Absolute time (CEST)	File time (m.s)	Distance (nm)
01/09/2023	Rigel III	Passenger	41°16’28.9’’N;019°22’26.7’’E	08:37	0	start rec.
01/09/2023	Rigel III	Passenger	41°16’28.9’’N; 019°22’26.7’’E	08:39	2.01	0.97
01/09/2023	Rigel III	Passenger	41°16’28.9’’N; 019°22’26.7’’E	08:39	2.24	0.83
01/09/2023	Rigel III	Passenger	41°16’28.9’’N; 019°22’26.7’’E	08:40	3.06	0.77
01/09/2023	Rigel III	Passenger	41°16’28.9’’N; 019°22’26.7’’E	08:40	3.46	0.64
01/09/2023	Rigel III	Passenger	41°16’28.9’’N; 019°22’26.7’’E	08:41	4.18	0.61
01/09/2023	Rigel III	Passenger	41°16’28.9’’N; 019°22’26.7’’E	08:41	4.49	0.6
01/09/2023	Rigel III	Passenger	41°16’28.9’’N; 019°22’26.7’’E	08:42	5.09	0.64
01/09/2023	Rigel III	Passenger	41°16’28.9’’N; 019°22’26.7’’E	08:43	6.02	0.72
01/09/2023	Rigel III	Passenger	41°16’28.9’’N; 019°22’26.7’’E	08:43	6.3	0.85
01/09/2023	Rigel III	Passenger	41°16’28.9’’N; 019°22’26.7’’E	08:44	7.02	stop rec.
01/09/2023	Francesca	Passenger	41°16’55.2’’N; 019°22’22.1’’E	10:03	0	start rec.
01/09/2023	Francesca	Passenger	41°16’55.2’’N; 019°22’22.1’’E	10:05	0.58	3.24
01/09/2023	Francesca	Passenger	41°16’55.2’’N; 019°22’22.1’’E	10:07	2.35	2.9
01/09/2023	Francesca	Passenger	41°16’55.2’’N; 019°22’22.1’’E	10:08	3.06	2.68
01/09/2023	Francesca	Passenger	41°16’55.2’’N; 019°22’22.1’’E	10:08	4.07	2.53
01/09/2023	Francesca	Passenger	41°16’55.2’’N; 019°22’22.1’’E	10:10	5.16	2.3
01/09/2023	Francesca	Passenger	41°16’55.2’’N; 019°22’22.1’’E	10:11	6.41	2.1
01/09/2023	Francesca	Passenger	41°16’55.2’’N; 019°22’22.1’’E	10:12	7.48	2
01/09/2023	Francesca	Passenger	41°16’55.2’’N; 019°22’22.1’’E	10:13	8.47	1.92
01/09/2023	Francesca	Passenger	41°16’55.2’’N; 019°22’22.1’’E	10:14	9.36	1.88
01/09/2023	Francesca	Passenger	41°16’55.2’’N; 019°22’22.1’’E	10:15	10.51	1.8
01/09/2023	Francesca	Passenger	41°16’55.2’’N; 019°22’22.1’’E	10:17	11.46	1.85
01/09/2023	Francesca	Passenger	41°16’55.2’’N; 019°22’22.1’’E	10:17	12.41	1.86
01/09/2023	Francesca	Passenger	41°16’55.2’’N; 019°22’22.1’’E	10:18	13.28	1.94
01/09/2023	Francesca	Passenger	41°16’55.2’’N; 019°22’22.1’’E	10:19	14.03	Stop rec.

Table 7. Information on location, time recording and distances from the listening station and the ferry.

5.4. Data analysis

Data analysis and charts were made with Matlab, Raven Pro 1.6 and R (version 4.3.1).

5.4.1. Acoustic parameters

Acoustic parameters which were used to describe noise are:

- Sound pressure level broadband ($L_{p,rms}$). It was calculated using a time-window of 10s, which was taken around CPA for the two ferries and in a random interval for the Blank.
- Sound pressure level ($L_{p,rms}$) for the one-third-octave bands of 63,125, 250 and 500 Hz. Bands of 63 and 125 Hz were chosen following the indication of Marine Strategy Framework Directive. Bands of 250 and 500 Hz were considered for further detail. For each one of the acoustic files (i.e. for Rigel III, AF Francesca and the Blank) and for each one-third-octave band, measurements on a time window of 10s were made. For both ferries they were taken in time intervals corresponding to the known distances, so that for each acoustic measurements that we have, we know the exact distance from the receiver and the source. For the Blank, 10 randomly measures were chosen. In all three cases, the results were reported as average values.
- Power spectral density (PSD). Calculated using time-windows of 1s, considering 10 adjacent measures around the CPA.
- Propagation loss (PL), which is a function of sound speed, temperature, bathymetry and bottom type (reported in dB).

When considering sound pressure level broadband and power spectral density, calculations were done once considering the original files and once applying a further high-pass filter at 10 Hz, in addition to the high-pass applied to the recordings during their acquisition. Such filter was applied to the acoustic files before the analysis in Matlab.

5.4.2. Modelling

Choosing the best model for propagation loss is based on the considerations of several factors. First, we have to distinguish between deep and shallow water. To understand local environment, we downloaded bathymetries from the software Global Mapper (Table 8). We considered a transect in the direction East-West of the study area. Measurements were taken at steps of 100 m.

Steps (m)		Depth (m)
0	0	42
1	100	43
2	200	44
3	300	45
4	400	46
5	500	47
6	600	48
7	700	49
8	800	50
9	900	51
10	1000	52

Table 8. Values of bathymetry data of the study area collected from Global Mapper.

We are in shallow water conditions. Typical shallow water environments are found on the continental shelf for water depths down to 200 m (Jensen *et al*., 2011).

Another discriminant factor is frequency, i.e. low or high (Cefas, 2015). Since we are modelling shipping noise we are dealing with low frequency (< 1000 Hz). In this study we consider one-third-octave bands centred at 63, 125, 250 and 500 Hz. Lower and upper limits are reported in Table 9.

Lower limit (Hz)	Centre frequency (Hz)	Upper limit (Hz)
56.2	**63**	70.8
112	**125**	141
224	**250**	282
447	**500**	562

Table 9. Limits and centre frequency of one-third-octave bands used in this study.

The final choice fell on RAMsGeo (Parabolic equation), according to previous cited characteristics and the environment type: range dependent and sandy to muddy bottom (Figure 12). This operation was done following (Cefas, 2015). The propagation model was elaborated using the package AcTUP v.2.2 (https://oalib-acoustics.org/models-and-software/parabolic-equation/)

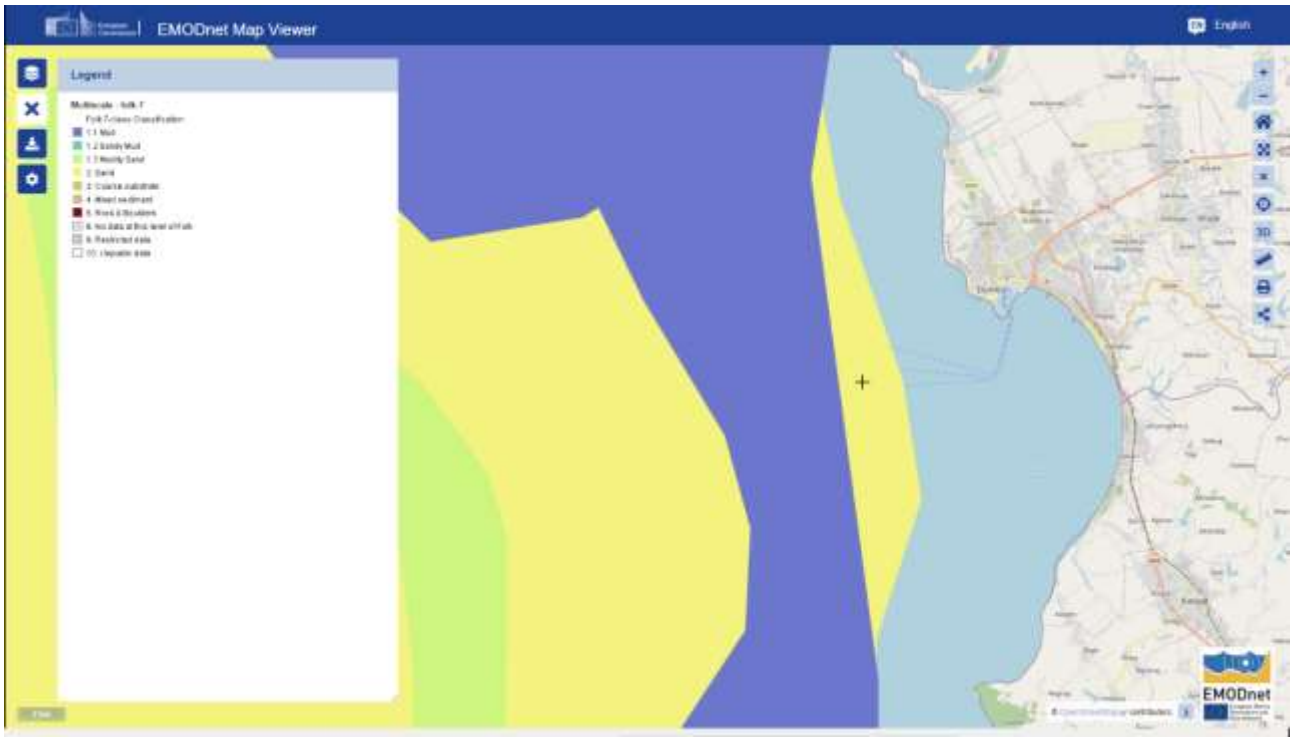

Figure 12. Figure showing sediment type in the study area (identify by a cross). Derived from EMODnet map viewer (https://emodnet.ec.europa.eu/geoviewer/#!).

Parameters which were used to build the model are:

- Speed sound (courtesy of JASCO): 1537 m/s;
- Bottom loss: c_p=1650 m/s (Jensen *et al*., 2011)

The compressional wave speed (c_p) was taken from Jensen *et al*., 2011. A list of the complete useful parameters when considering bottom loss is reported in Table 10.

Bottom type	P (%)	ρ_b/ρ_w	c_p/c_w	c_p(m/s)	c_s (m/s)	α_p (dB/λ_p)	α_s (dB/λ_s)
Sand	45	1.9	1.1	1650	$110_z{}^{\sim 0.3}$	0.8	2.5
silt	55	1.7	1.05	1575	$80_z{}^{\sim 0.3}$	1.0	1.5

Table 10. Geoacoustic properties of continental shelf and slope environments. From Jensen et al., 2011.

6. Results

Figure 13 shows the spectrogram of Rigel III during the closest point of approach. This is the moment of major acquired noise, since the distance between the receiver and the ship is minimum.

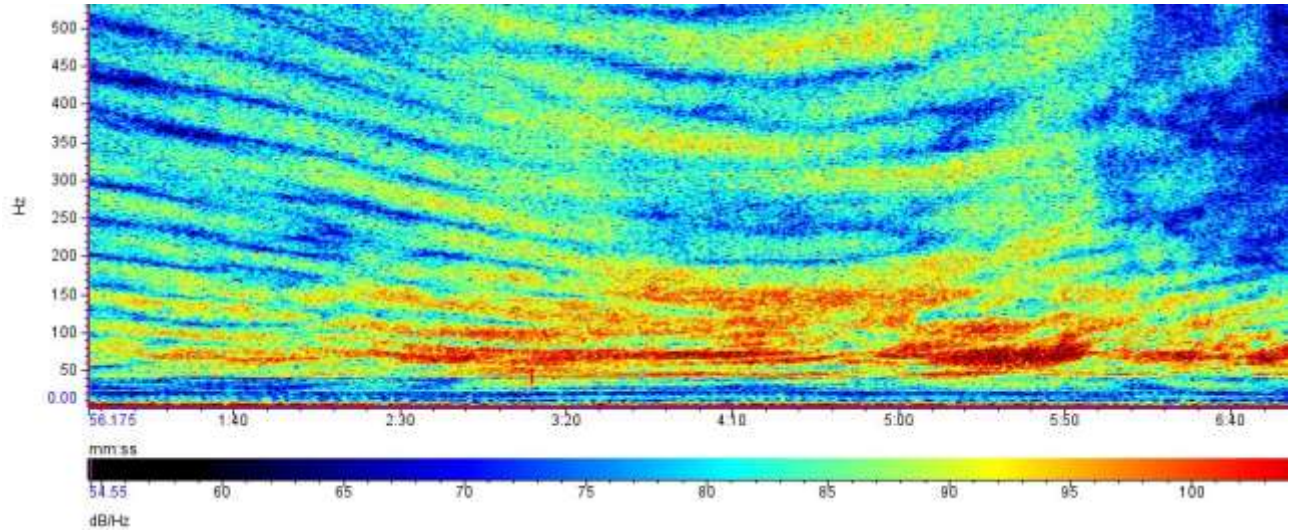

Figure 13. Spectrogram of CPA of Rigel III

6.1. Values of acoustic parameters

Figures of power spectral density for Rigel III (Figures 14-15), AF Francesca (Figures 16-17) and the Blank (Figure 18-19) are reported. For each of the three elements we calculated the PSD both with and without an additional high-pass filter at 10 Hz.

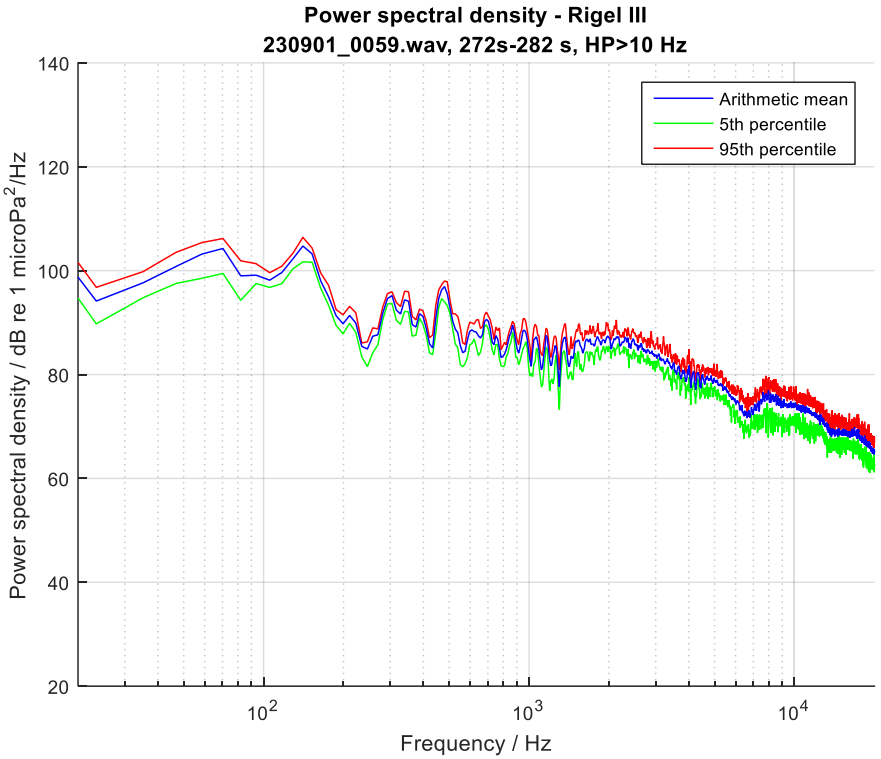

Figure 14. Power spectral density for CPA of Rigel III, taking into account an additional high-pass filter at 10 Hz.

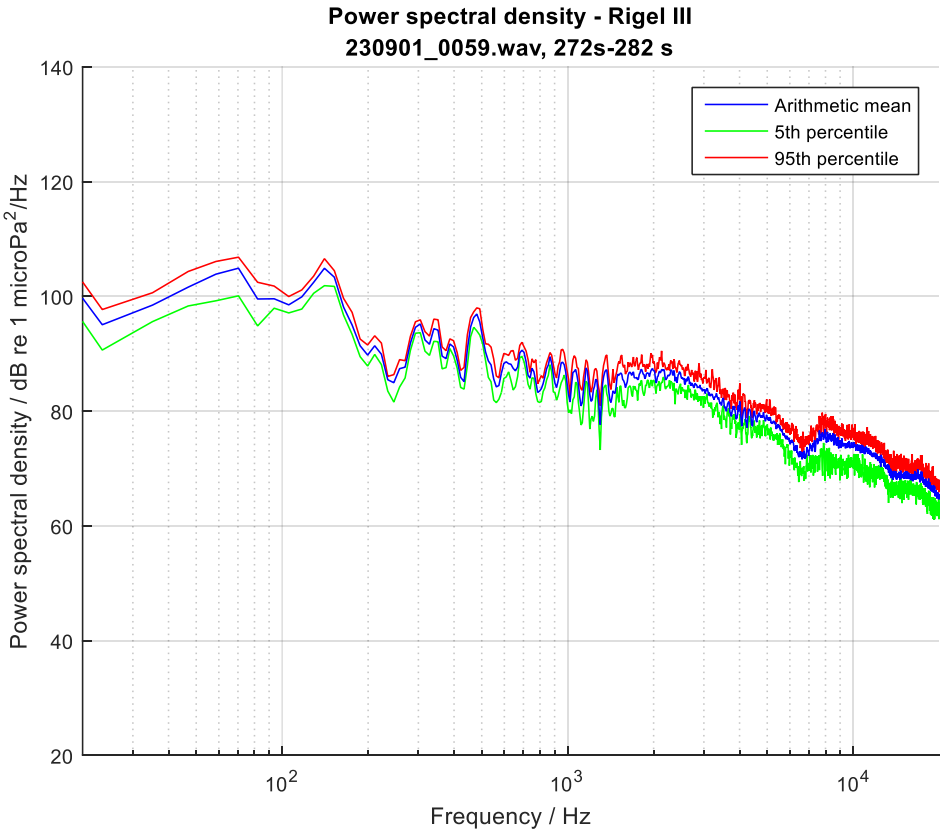

Figure 15. Power spectral density for CPA of Rigel III.

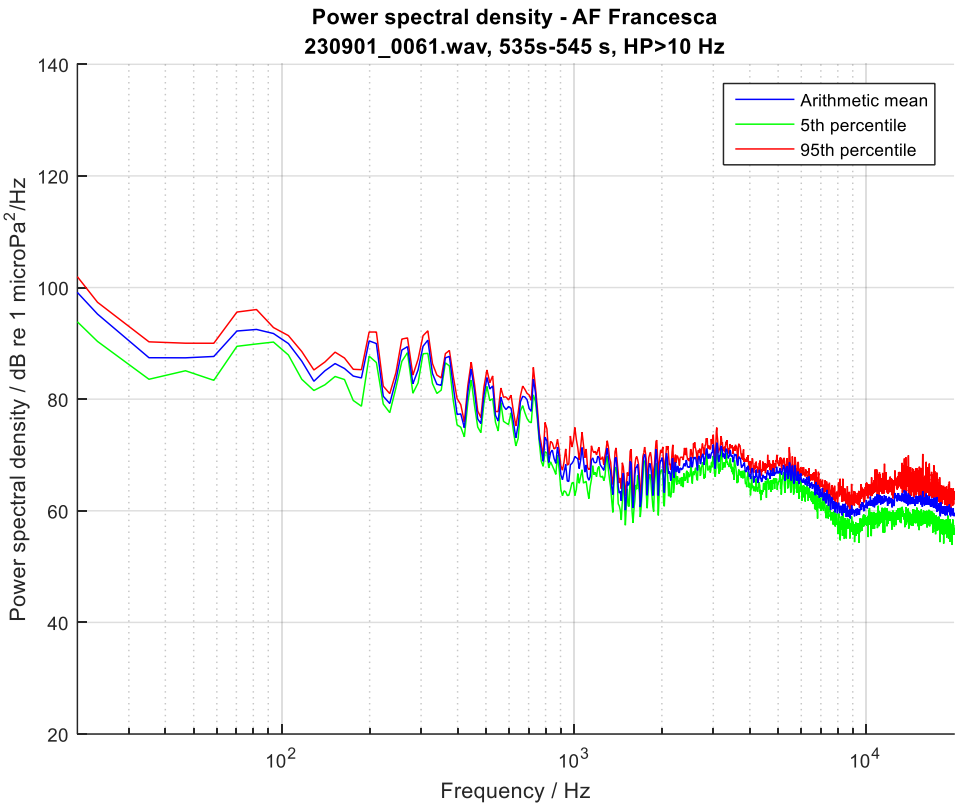

Figure 16. Power spectral density for CPA of AF Francesca, taking into account an additional high-pass filter at 10 Hz.

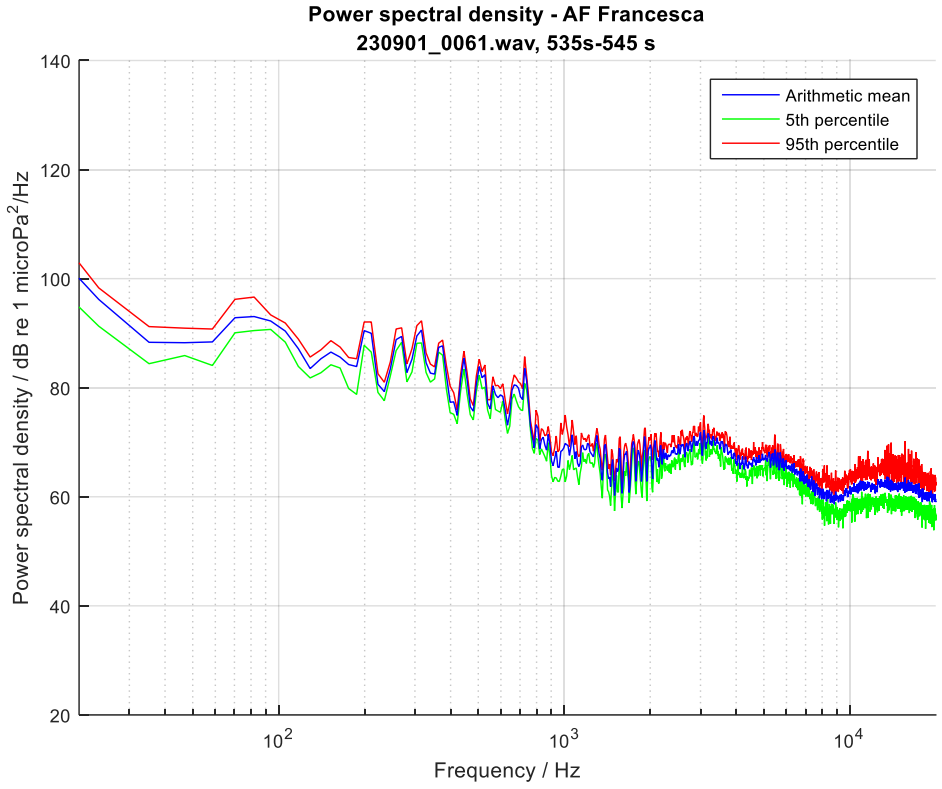

Figure 17. Power spectral density for CPA of AF Francesca.

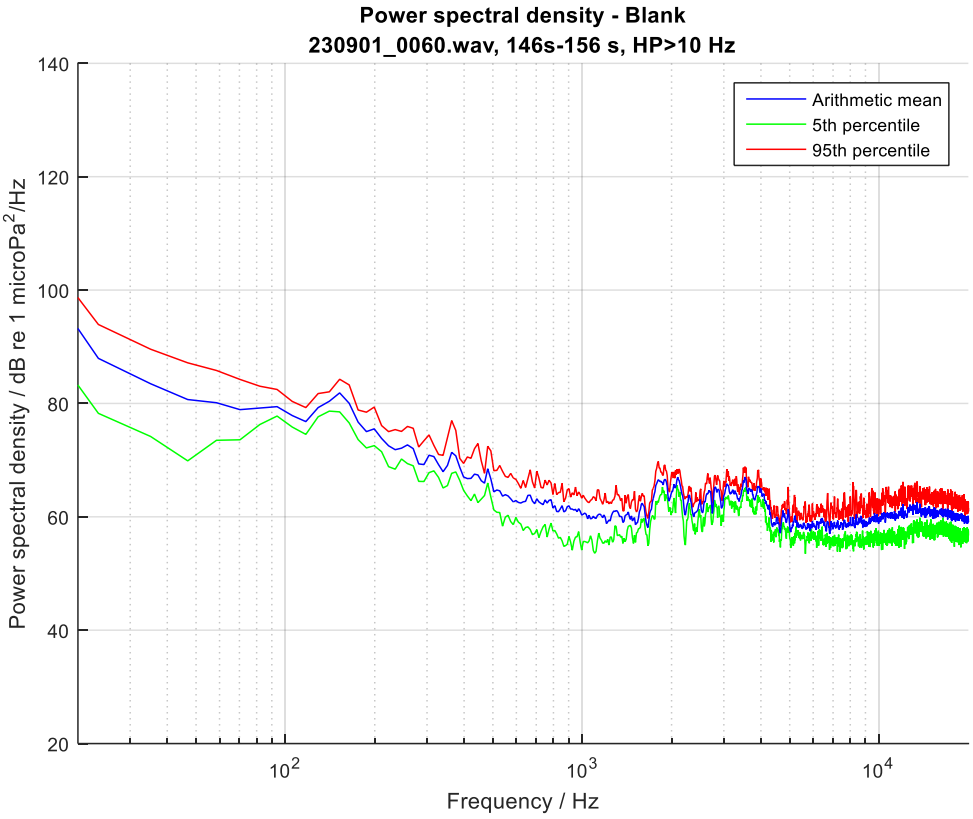

Figure 18. Power spectral density for the Blank, taking into account an additional high-pass filter at 10 Hz.

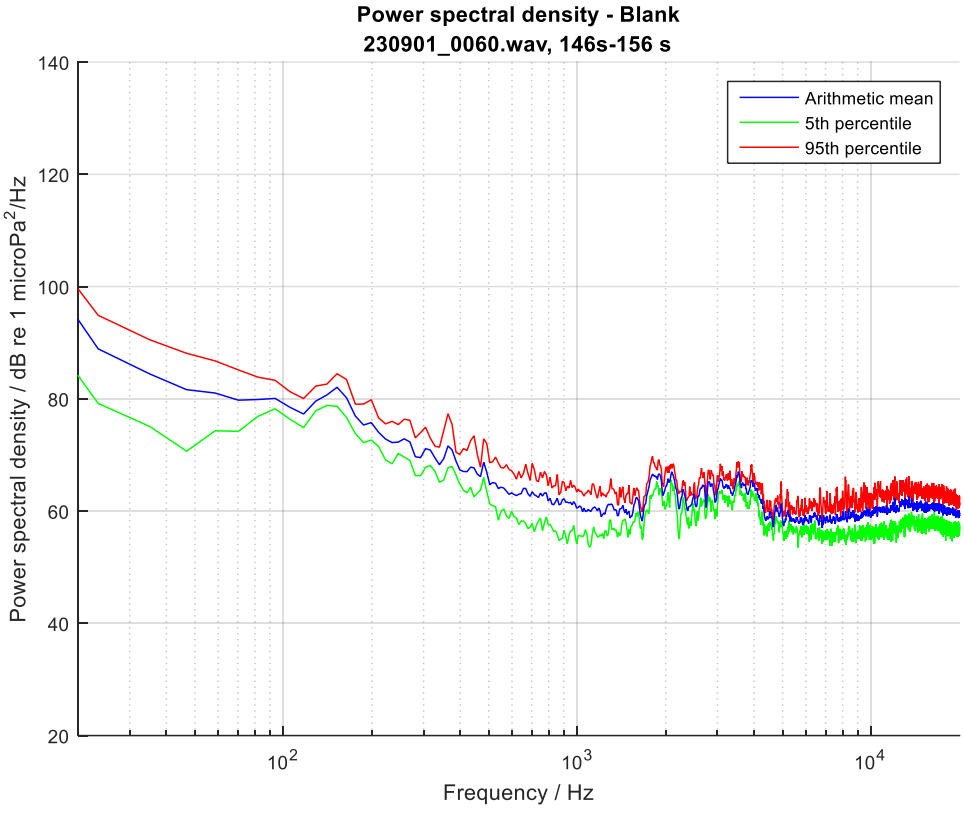

Figure 19. Power spectral density for CPA of the Blank.

Figure 20 reports values of $L_{p,rms}$ for the one-third-octave bands of 63, 125, 250 and 500 Hz.

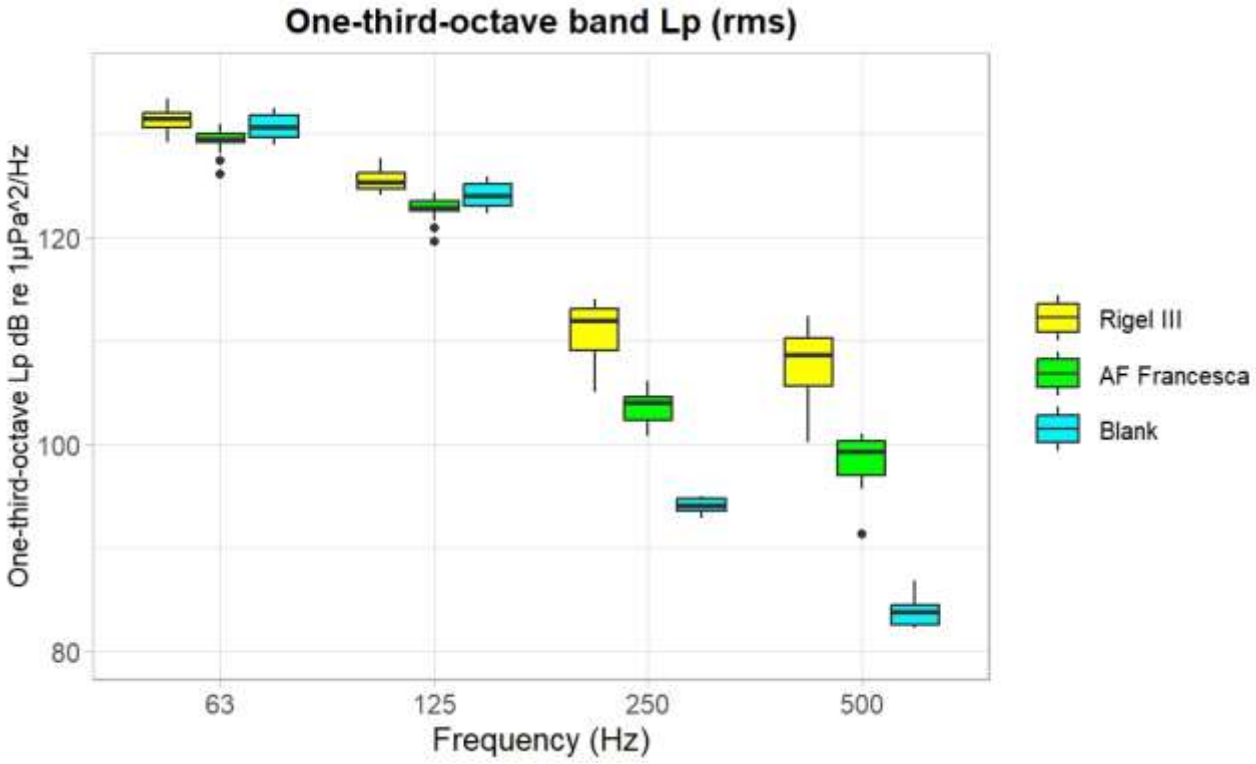

Figure 20. Figure showing measurements of $L_p(rms)$ in one-third octave bands of 63, 125, 250, 500 Hz during the passage of Rigel III and AF Francesca as well as for the "blank".

Measures of $L_{p,rms}$ broadband for a time window of 10s are reported in Table 11. For the ferries Rigel III and AF Francesca measurements were done at CPA, while for the Blank a time window was randomly chosen.

What	High-pass filter	Time window	L_p (dB re 1µPa)
Rigel III	yes	10 s (CPA)	131.6481
Rigel III	no	10 s (CPA)	132.4152
AF Francesca	yes	10 s (CPA)	128.3859
AF Francesca	no	10 s (CPA)	129.3106
Blank	yes	10 s	127.4287
Blank	no	10 s	128.3793

Table 11. Table reporting values of L_p broadband for Rigel III, AF Francesca and Blank.

6.2. Modelling

Modelling propagation loss up to 1000 m away from the noise source, showed that we deal with near-cylindrical spreading. Spreading loss is simply a measure of the signal weakening as it propagates outward from the source. When the medium has plane upper and lower boundaries as in the waveguide case in Figure 21, the far field intensity change with horizontal range becomes inversely proportional to the surface of a cylinder of radius R and depth D (Jensen *et al*., 2011). Cylindrical spreading loss is therefore given by

$$TL = 10logr \ \ (dB\ re\ 1m)$$

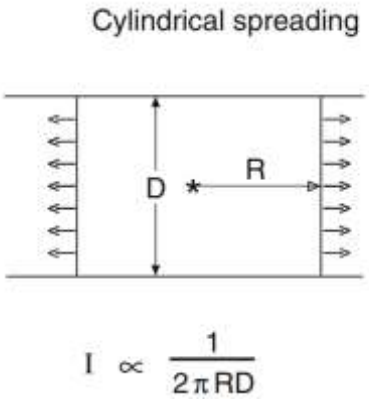

Figure 21. Geometrical spreading low. From Jenset et al. (2011).

Propagation loss

In order to identify the area potentially impacted by sound, propagation loss (PL) must be determined. The sonar equation (Urick, 1983) RL = SL - PL (RL= Received Level, SL = Source Level, PL= Propagation Loss) determines PL = SL – RL. If the range between source and receiver is known, reasonable predictions of PL are given by the formula PL = N log_{10}(R), (N = scaling factor, R= range).

A common practice is to define spherical spreading as 20log(R) and cylindrical spreading 10log(R). Brekhovskikh (1965) and Weston (1971) define 15log(R) as “intermediate spreading” or “practical spreading”.

Figure 22 shows spreading prediction for parameters of Durrës, a source at 5m depth and f=125Hz.

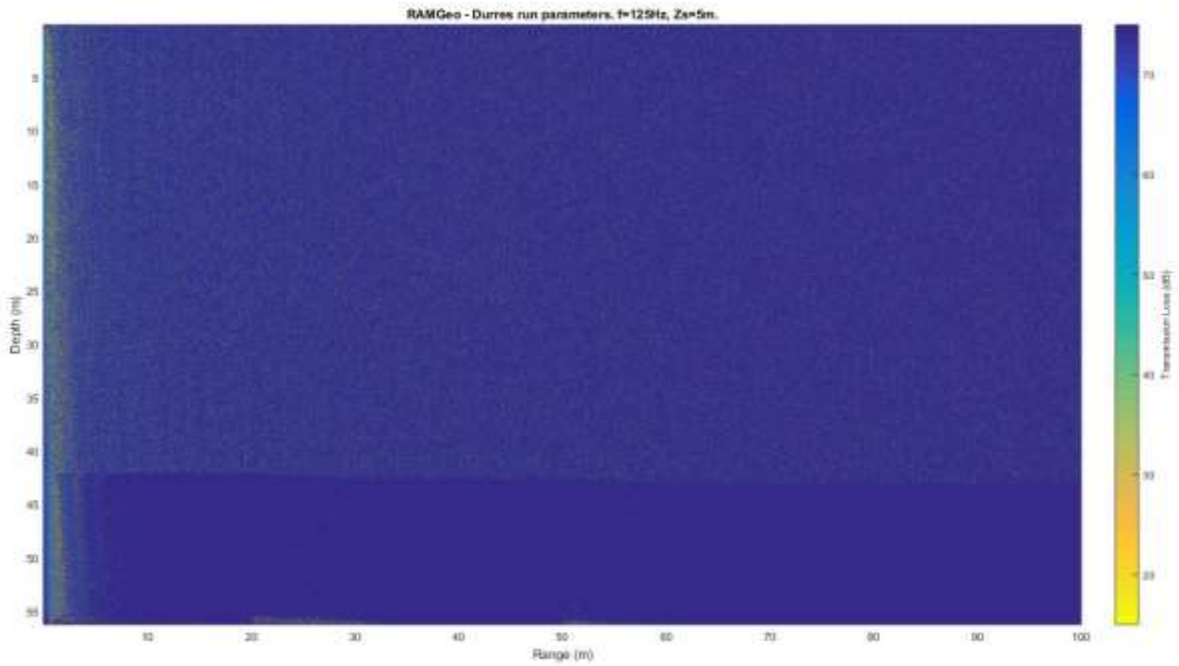

Figure 22. Figure showing spreading prediction for parameters of Durrës, a source at 5m depth and f=125Hz.

Measurements (Table 12) confirm that, for the frequencies within the one-third-octave band centered at 125 Hz, propagation loss between our receiver and Rigel III, and our receiver and AF Francesca, is approximately 15log(R).

Ship	Speed (knts)	Distance at CPA (m)	Center frequency TOB (Hz)	Expected SL (dB re 1µPa m)	PL=10logR (dB)	PL=15logR (dB)	(10logR) Expected RL (dB re 1 µPa)	(15logR) Expected RL (dB re 1 µPa)	Measured RL at CPA (dB re 1 µPa)	Measured PL (dB)
Rigel III	13.4	1111	63	171.04	30	46	141.04	125.04	130	41
Rigel III	13.4	1111	125	173.05	30	46	143.05	**127.05**	**125**	**48**
Rigel III	13.4	1111	250	172.53	30	46	142.53	126.53	113	60
Rigel III	13.4	1111	500	169.96	30	46	139.96	123.96	112	58
AF Francesca	12.9	3334	63	170.78	35	53	135.78	117.78	126	45
AF Francesca	12.9	3334	125	172.79	35	53	137.79	**119.79**	**120**	**53**
AF Francesca	12.9	3334	250	172.27	35	53	137.27	119.27	104	68
AF Francesca	12.9	3334	500	169.7	35	53	134.7	116.7	100	70

Table 12. Table reporting values of a) expected Source Level (SL) of Rigel III and AF Francesca according to MacGillivray & de Jong (2021) for the one-third-octave bands (TOB) of 63, 125, 250 and 500 Hz, b) propagation Loss (PL) according to the formula PL=101ogR and PL=15logR, c) expected Received Level (RL) following the previous formulas, d) Received Levels that were actually measured with our hydrophone.

7. Discussion

Our results, if compared with literature (e.g. the Wenz curves; Figure 23), show broadband sound pressure levels $L_{p,rms}$ ranging from 129-132 dB re 1µPa while ships are underway, and 127-128 dB re 1µPa with no ships underway in the range of 5000m. Spectral density of ships underway peaks at approximately 100-110 dB re 1µPa^2/Hz, while ambient "Blank" is at levels where Wenz places heavy shipping noise. Hence the location can be defined as "noisy".

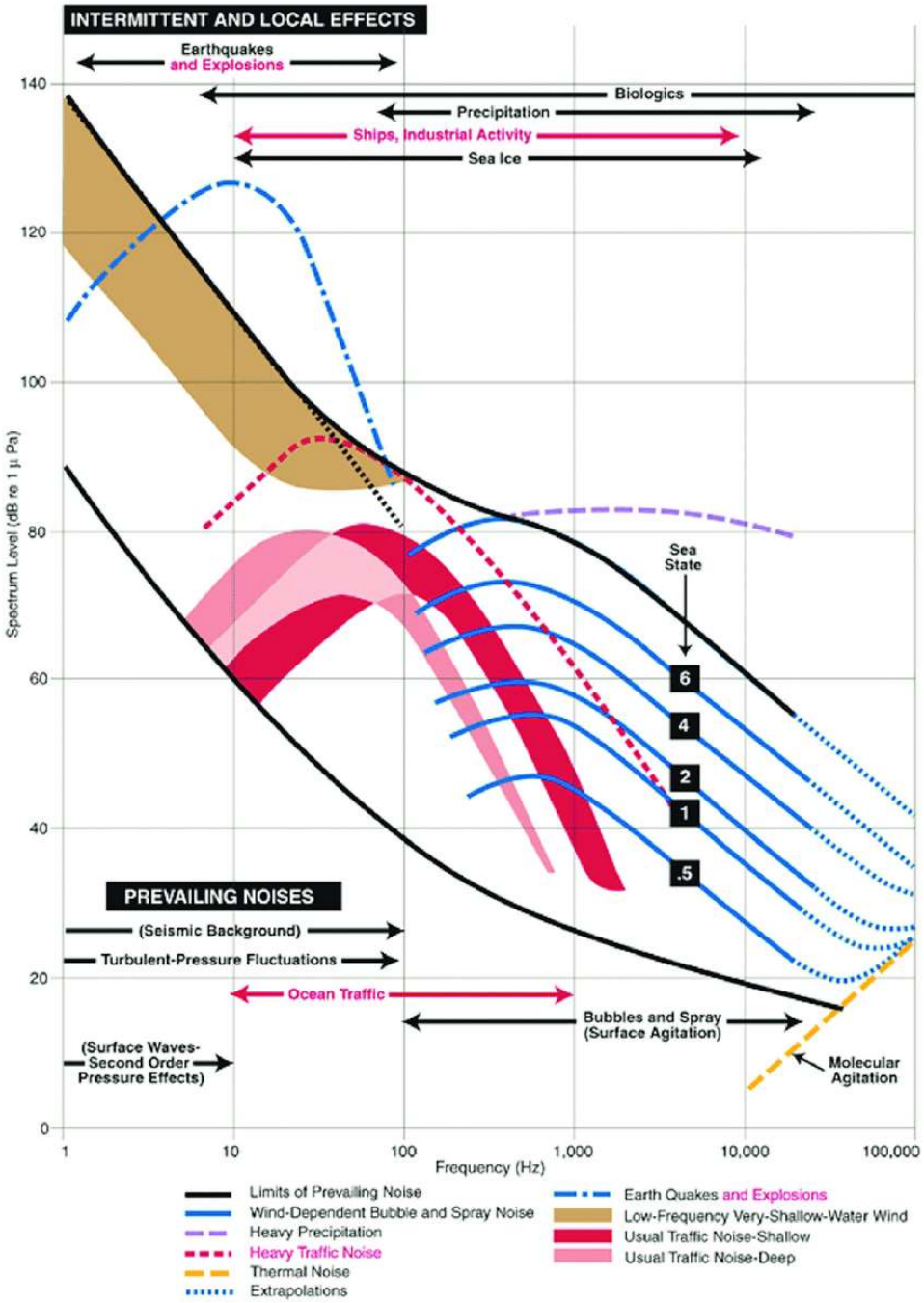

Figure 23. Wenz curves describing power spectral density levels of marine ambient noise derived from weather, wind, geologic activity, and commercial shipping. (Adapted from Wenz, 1962.). From Affatati (2020).

Shipping noise is known to potentially impact fish and invertebrates in different ways and degrees of severity. Among the commercially exploited species in the Adriatic Sea, there are: a gadoid fish, the European Hake (*Merluccius merluccius*), a crustacean, the Norway lobster (*Nephrops norvegicus*) as well as a mollusc, the common cuttlefish, (*Sepia officinalis*).

Gadoid fish sounds (Figure 23 for audiograms) are masked by changes in ambient background noise (Figure 24) (Hawkins & Chapman, 1975) and which may affect spawning behavior (Hawkins & Picciulin, 2019). Further larval growth is affected for gadoids exposed to shipping noise (Nedelec *et al*., 2015). Among crustaceans, while studies on the Norway lobster do not relate it directly to shipping noise rather than to particle motion (Goodall *et al*., 1990), relatives of it such as the spiny lobster and the common prawn show changes in locomotory pattern and clear indicators of stress (Filiciotto *et al*., 2014; Filiciotto *et al*., 2016).

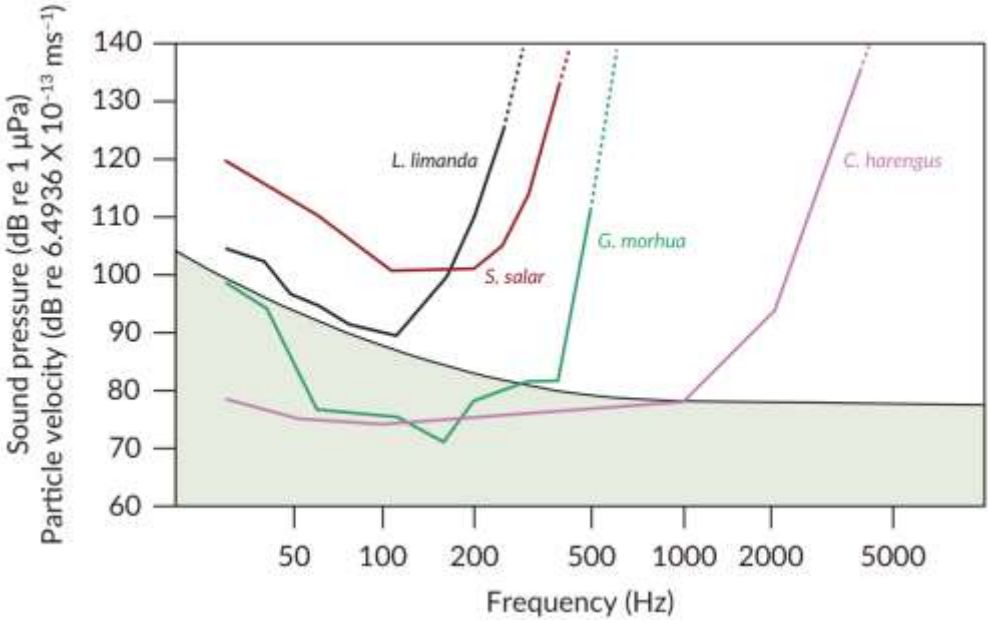

Figure 23. Fish hearing sensitivity (thresholds) for four species of fish; the dab Limanda limanda (Chapman and Sand, 1974); the Atlantic salmon Salmo salar (Hawkins and Johnstone (1978); the Atlantic cod Gadus morhua (Chapman and Hawkins, 1973); and the Atlantic herring Clupea harengus (Enger, 1967). From Popper & Hawkins (2019)

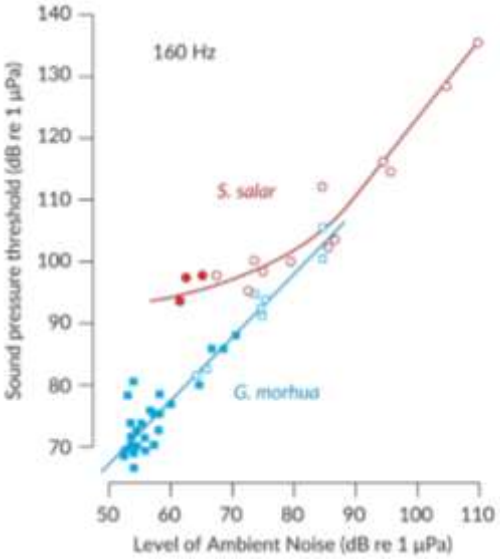

Figure 24. Masking of Gadus morhua and Salmo salar by ambient noise. The thresholds were determined using a pure tone signal at a frequency of 160 Hz. Ambient noise (natural sea noise, augmented by white noise from a loudspeaker) is expressed as the spectrum level at that same frequency (dB re 1 µPa/Hz). Closed symbols:thresholds to natural levels of ambient noise; open symbols: thresholds to anthropogenic noise. n.b., The thresholds in S. salar were only influenced by noise levels above the natural ambient levels of noise (data from Hawkins, 1993). From Popper & Hawkins (2019)

Samson *et al*. (2014) reports consistent changes in behavior in the common cuttlefish. In particular, graded behavioral responses to different frequencies and sound pressure level are observed. Figure 25 summarizes their results.

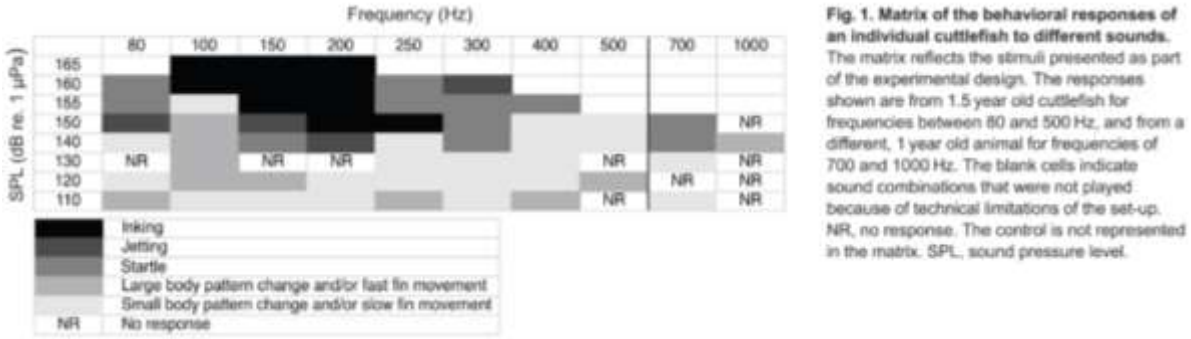

Fig. 1. Matrix of the behavioral responses of an individual cuttlefish to different sounds. The matrix reflects the stimuli presented as part of the experimental design. The responses shown are from 1.5 year old cuttlefish for frequencies between 80 and 500 Hz, and from a different, 1 year old animal for frequencies of 700 and 1000 Hz. The blank cells indicate sound combinations that were not played because of technical limitations of the set-up. NR, no response. The control is not represented in the matrix. SPL, sound pressure level.

Figure 25. Behavioural responses of common cuttlefish to diverse sound stimuli. From Samson et al. (2014).

8. Conclusions

Durrës Bay presented high levels of ambient noise. Due to local oceanographic conditions sound propagated with low attenuation in an intermediate spreading mode. Levels, duration and repetition patterns of irradiated noise suggested that no direct physical harm to fish can be foreseen. However, for three commercial species, namely the Hake, the Norway lobster and the common cuttlefish,

reactions and physiological consequences related to stress can be predicted. With the necessity of finding both temporal and spatial mitigation options, we suggest that a precise corridor for entry and leave routes for ships is defined and that when possible, speed reduction is applied within a range of 5000m from Durrës Harbour.

9. Literature

Affatati, A. (2020). Underwater noise in the marine environment: Sources, effects on fauna and mitigation measures| Rumore subacqueo in ambiente marino: Fonti, effetti sulla fauna e misure di mitigazione. Bollettino di Geofisica Teorica ed Applicata. http://dx.doi.org/10.4430/bgta0323

Brekhovskikh, L.M., 1965. The average field in an underwater sound channel. Sov. Phys. Acoust. 11, 126–134

Cefas (2015). Impacts of noise and use of propagation models to predict the recipient side of noise. Report prepared under contract ENV.D.2/FRA/2012/0025 for the European Commission. Centre for Environment, Fisheries & Aquaculture Science, UK

Dekeling, R.P.A., Tasker, M.L., Van der Graaf, A.J., Ainslie, M.A, Andersson, M.H., André, M. et al. (2014). Monitoring Guidance for Underwater Noise in European Seas, Part II: Monitoring Guidance Specifications, JRC Scientific and Policy Report EUR 26555 EN, Publications Office of the European Union, Luxembourg https://dx.doi.org/10.2788/27158

Duarte, C. M., Chapuis, L., Collin, S. P., Costa, D. P., Devassy, R. P., Eguiluz, V. M., ... & Juanes, F. (2021). The soundscape of the Anthropocene ocean. Science, 371(6529), eaba4658. https://doi.org/10.1126/science.aba4658

Filiciotto, F., Vazzana, M., Celi, M., Maccarrone, V., Ceraulo, M., Buffa, G., Arizza, V., de Vincenzi, G., Grammauta, R., Mazzola, S., and Buscaino, G. (2016). Underwater noise from boats: Measurement of its influence on the behaviour and biochemistry of the common prawn (Palaemon serratus, Pennant 1777). J. Exper. Mar. Biol. Ecol. 478: 24-33.

Filiciotto, F., Vazzana, M., Celi, M., Maccarrone, V., Ceraulo, M., Buffa, G., Di Stefano, V., Mazzola, S., and Buscaino, G. (2014). Behavioural and biochemical stress responses of Palinurus elephas after exposure to boat noise pollution in tank. Mar. Poll. Bull. 84 (1-2): 104-114.

Jensen, F. B., Kuperman, W. A., Porter, M. B., Schmidt, H., & Tolstoy, A. (2011). Computational ocean acoustics (Vol. 2011). New York, NY: Springer New York. https://doi.org/10.1007/978-1-4419-8678-8

Hawkins, A. D., and Chapman, C. J. (1975). “Masked auditory thresholds in the cod, Gadus morhua L,” J. Comp. Physiol. 103, 209–226.

Hawkins, A. D., & Picciulin, M. (2019). The importance of underwater sounds to gadoid fishes. The Journal of the Acoustical Society of America, 146(5), 3536-3551.

ISO 18405:2017. Underwater acoustics - Terminology, International Organization for Standardization (ISO, Geneva, Switzerland). Available from: http://www.iso.org/iso/catalogue_detail.htm?csnumber=62406

ISO 13261-2:1998. Sound power rating of air-conditioning and air-source heat pump equipment. Part 2: Non-ducted indoor equipment, International Organization for Standardization (ISO, Geneva, Switzerland). Available from: https://www.iso.org/standard/27294.html

MacGillivray, A., & de Jong, C. (2021). A reference spectrum model for estimating source levels of marine shipping based on Automated Identification System data. Journal of Marine Science and Engineering, 9(4), 369. https://doi.org/10.3390/jmse9040369

Nedelec, S.L., Simpson, S.D., Morley, E.L., Nedelec, B., and Radford, A.N. 2015. Impacts of regular and random noise on the behaviour, growth and development of larval Atlantic cod (Gadus morhua). Proc. R. Soc. B 282 (1817): 20151943

Popper, A. N., & Hawkins, A. D. (2019). An overview of fish bioacoustics and the impacts of anthropogenic sounds on fishes. Journal of fish biology, 94(5), 692-713. https://doi.org/10.1111/jfb.13948

Samson, J. E., Mooney, T. A., Gussekloo, S. W., & Hanlon, R. T. (2014). Graded behavioral responses and habituation to sound in the common cuttlefish Sepia officinalis. Journal of Experimental Biology, 217(24), 4347-4355.

Urick, R.J., 1983. Principles of Underwater Sound. third ed. McGraw-Hill, NY.

Weston, D.E., 1971. Intensity–range relations in oceanographic acoustics. J. Sound Vib. 18, 271–287. http://dx.doi.org/10.1016/0022-460X(71)90350-6.